Indian Journal of Engineering & Materials Sciences
Vol. 28, February 2021, pp. 64-72

Examining the effect of nano-additions of rare earth elements on the hardness of body armor ceramic

Mohammad Shbool[*a], Yousef Al-Abdallat[a], Abdul Kareem Abdul Jawwad[a], Saja Alsharairi[a], Leen Abu-Ghannam[a], Ezz-Eddin Abu-Khajil[a] & Ahmad Badwan[b]

[a]Industrial Engineering Department, The University of Jordan, Amman 11942, Jordan

[b]IAE Aix-Marseille Graduate School of Management, Aix-Marseille Université, France

Received: 11 September 2019; Accepted: 17 February 2020

Body armor is a very critical entity in protecting soldier's live. Soldiers carry heavy stuff on duties, and the ceramic insert in those body armors is one of them. The purpose of this paper is to investigate the effect of Nano-rare-earth elements as additives to the ceramic base material on the armor's performance. Aluminum oxide (Al_2O_3) has been selected as the base material of the ceramic in this study. This study has chosen two additives: Zirconium dioxide (ZrO_2) and Nano-ceramic lab composite (NCLC). In this work, we have presented results of mechanical characterization for alumina-nanocomposites armor plates. Three different concentrations of NCLC and ZnO_2 alumina-based compositions have been prepared and pressed at 40 and 50 MPa and sintered at 1350°C for 120 min. X-ray diffraction and scanning electron microscopy (SEM) techniques have been employed to characterize structural, morphological, and phase identification of the films. Mohs test hardness measurements of samples after sintering have been performed. Results have shown that the compositions with NCLC showed a higher hardness than a composition with ZrO_2. This result has indicated that the addition of NCLC to Alumina enhances the microstructure and increases the ceramics' hardness.

Keywords: ANOVA, Body armor, Hardness, Nanocomposites

1 Introduction

In today's military context, body armor gear is considered a crucial necessity while at the same time placinga "weight penalty" due to the heavyweight of this life-saving piece. Several body armors with different designs and materials are available depending on the required level of protection and other functional attributes. Improved body armor in enhanced protection and lighter weight is the primary focus for military research, according to National Research Council[1]. Further studies were devoted to the flexible layer of the body armor. For example, Benzait[2] reviewed recently published research on materials utilized in the body armor's polymer-matrix composites. Their study's purpose was the same as ours, investigating materials that enhance the body armor's performance. Still, they focused on the flexible layer, and our focus is on the ceramic insert.

Heavy-duty body armors use metallic or ceramic protective plate-insert in their bullet-resistant vests. The insert provides extra protection from rifle rounds with tightly woven fibers such as Kevlar. Medvedovski[3] focused on the ceramic insert. The ceramic structure, especially the alumina-ceramic, its manufacturing features and properties that enhance energy dissipation capability make ceramics suitable for ballistic protection. The ceramic materials' essential property" the strong covalent bonding between lightweight atoms located in the first quarter of the periodic table of elements, "which makes them appropriate for ballistic protection (National Research Council[1]). According to McCauley[4], oxides ceramics are mostly preferred because of their cost relative to performance, with Al_2O_3being the most developed among other ceramic-based materials (National Research Council[1]). According to Lamba[5], Alumina ceramics are widely used in different heavy-duty applications, like the vacuum-tight seals, to develop 5 MW klystron.

Ceramic armor inserts absorb the projectile kinetic energy through the fracture, unlike the metallic armor mechanism, which results in plastic deformation, Medvedovski[6]. Hence, ceramic armor is used as an insert covered with a high tensile strength layer of polymeric fibers, such as Kevlar™, Twaron™, Spectra™, and Dyneema™. Crouch[7] did a study on the mild-steel-cored ammunition's penetration behavior against armors made of ceramics. This research focuses

*Corresponding author (E-mail: m.shbool@ju.edu.jo)

on the heaviest piece of the armor; the ceramic insert. The purpose was to improve the insert's performance given the same weight of current inserts or reducing the weight given the same performance or both. The Ceramic used in the study was Al_2O_3-4wt%Nb_2O_5. Both ballistic simulation and actual testing of the high velocity 7.62 mm ammunition showed that the convex-curved surface outperforms the flat surface ceramics by 16-18%. Our current research intends to investigate new additives to enhance armor ceramic performance rather than designs.

In multilayered armors, a front ceramic plate can dissipate more than 50% of the impact energy, and investigations continuously attempt to increase this performance. For the first time, this communication revealed how much impact energy is dissipated in an Al_2O_3–4 wt%Nb_2O_5 convex-curved surface ceramic armor by high velocity 7.62 mm ammunition. Both ballistic simulation and actual tests indicate a 16–18% superior performance of the convex-curved surface compared to theflat surface ceramic.

The ceramic base material studied in this research is Aluminum Oxide (Al_2O_3). Alumina is still the most widely used Ceramic in body armor production due to its attractive properties relative to cost. According to Carter[8], Alumina combines good hardness and corrosion resistance with good strength and can be used in applications up to 1700°C. It is available in a range of purities with high purity ceramics (99.7%). For general properties and types of ceramics, see Groover[9]. An overview of ceramics for armor applications and their properties related to ballistic impact resistance was done by Karandikar[10]. They indicated that the role of hardness property in ballistic performance is the projectile's damage; this is the motivation for focusing on the hardness property in our current research.

In this study, Zirconium dioxide (ZrO_2) and nano-ceramic lab composite (NCLC) were used as additive materials to alumina-based material for body armor insert production. Nano-ceramic lab composite (NCLC), alight-curing composite resin filling with a high flow ability and elasticity, consisting of about 86% ceramic and 14% of polymer mixture. In recent years, the application of zirconia-based ceramics for dental restorations and dental implants has increased because of its high mechanical toughness, esthetics, and biocompatibility, Raigrodski[11]. Liang[12] studied the effect of isostatic pressing on producing high-density dental ceramics made of alumina and zirconia composite. The study concluded that sintering shrinkage was reduced through isostatic pressing. In general terms, the range of properties appealing to dental applications has a good deal of overlap with those required for body armor applications, including lightweight and high hardness, strength, and toughness levels. This similarity motivates the application of NCLC as an additive material in the present research in addition to zirconia.

This research aims to examine the effects of NCLC and zirconia concentrations under different processing conditions on the resulting structure and properties of alumina-based body armor insert components. This investigation has been accomplished by applying the statistical design of experiments (DOE) and the associated variance analysis (ANOVA).

2 Materials and experimental procedure

2.1 Preparation of the Nancomposites

Al_2O_3 powder (99.7% purity) was used for the base material, while different NCLC and ZrO_2 concentrations were added to Alumina under different pressure levels. The ranges of compositions and pressure levels are shown in Fig. 1. Al_2O_3 was milled using a vibratory mill for 15 min/100gram to obtain the powder in the smallest particle size possible. After milling, particles' size was screened using a sieve size of 63 μm. NCLC liquid-samples were dried using LED curing light for 30 seconds, based on Milosevic[13], and ground into

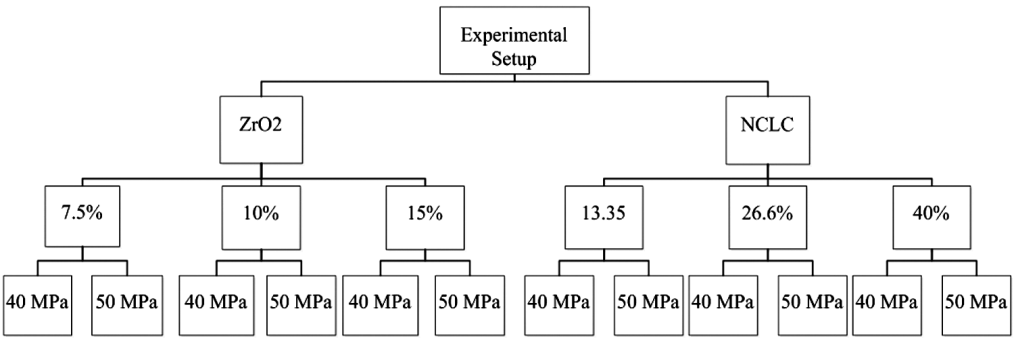

Fig. 1 — Factors and corresponding levels.

powder using a mortar grinder (RM 100 with grinding sets made of tungsten carbide). The ZrO_2 ground in the same way as the dried NCLC. After grinding, the corresponding concentrations of each additive material, as shown in Fig. 1, were added to the alumina base powder and pressed using the two pressure levels (40 MPa and 50 MPa) into cylindrical specimens of 25 mm diameter using a steel molding set and a hydraulic press. Before pressing, all mixtures were subject to a size screening using a sieve size of 63 µm. The cylindrical specimens were then sintered in a furnace at 1350°C for 120 minutes with a heating rate of 10°C/min without applying any pressure. Figure 2 below shows real images of the prepared specimens, where the dark one sample was dye for preparation to be tested in SEM.

2.2 Morphology

An FEI Quanta Thermo Scientific 200F SEM instrument was employed to perform SEM measurements in different magnifications. The scanning electron microscope produces a high-energy focused beam of electrons aimed at a solid sample surface. The interactions between electrons and samples generate signals that reveal information about the sample's chemical composition and external morphology. The field emission gun (FEG) system contains a STEM detector for bright and dark field sample imaging, which was also used.

2.3 Physical properties

The density and porosity of samples were calculated using the following equations (1-3) Mallick[14]:

$$\rho_{th} = \rho_m \times (\%\, of matrix) + \rho_r \times (\%\, of Reinforcement) \quad \ldots (1)$$

where,

ρ_m: $density of matrix$

ρ_r: density of reinforcement

ρ_{th}: theoretical density

$$Porosity of compact part = \frac{\rho_{th} - \rho_{exp}}{\rho_{th}} * 100\% \quad \ldots (2)$$

$$where, \rho_{exp} = \frac{mass}{volume} \quad \ldots (3)$$

ρ_{exp}: $experimental\ density$

The calculations of porosity, experimental and theoretical densities for all specimens are shown in Table 1. The hardness of the sample was evaluated using the Mohs test. The hardness collected data were statistically evaluated using the analysis of means, which was performed using Minitab software.

Fig. 2 — Specimens.

Table 1 — Samples densities and porosity.

Samples	Pressure	Sample ID	Theoretical density (g/cm^3)	Experimental density (g/cm^3)		Porosity percentage	
				Before sintering	After sintering	Before sintering	After sintering
ZrO_2 7.5%	40 MPa	1	4.0797	2.099	2.449	48.54%	39.97%
	50 MPa	2	4.0797	2.261	2.672	44.58%	34.50%
ZrO_2 10%	40 MPa	3	4.123	2.099	2.449	49.08%	40.60%
	50 MPa	4	4.123	2.261	2.672	45.16%	35.19%
ZrO_2 15%	40 MPa	5	4.2095	2.099	2.449	50.13%	41.82%
	50 MPa	6	4.2095	2.261	2.672	46.28%	36.52%
NCLC13.5%	40 MPa	7	4.123	2.099	2.449	49.09%	40.59%
	50 MPa	8	4.123	2.261	2.672	45.16%	35.10%
NCLC 16.6%	40 MPa	9	4.2968	2.099	2.449	51%	43%
	50 MPa	10	4.2968	2.261	2.672	47.37%	37.80%
NCLC 40%	40 MPa	11	4.4836	2.099	2.449	53.10%	45.30%
	50 MPa	12	4.4836	2.261	2.672	49.57%	40.40%

3 Results and Discussion

3.1 Surface analysis studies

Figure 3 shows the SEM micrographs of 30 µm and 10 µm magnifications of the Alumina–Zirconia composites with ZnO2 in 10% weight percent with respect to Alumina at two different pressure 40 MPa (A1, B1) and 50 MPA (A2, B2). Phase composition and microstructure of dense Alumina–zirconia ceramics consist of corundum grains as the major phase and a silicate-based glassy phase. Generally, the structure of the studied alumina ceramics is uniform and microcrystalline. The Alumina Ceramic's grain size depends on the initial batch composition, initial particle size, and particle size distribution of starting alumina powders. Alumina powders with a smaller particle and median crystal size provide a fine crystalline structure with smaller grain size. For Alumina–zirconia ceramics, the zirconia phase (about 500 nm grain size) is uniformly distributed among alumina grains with sizes of 1– 6 µm (Fig. 3). The smaller ZrO_2 particles seem to be entrapped within the alumina grains, and the larger ZrO_2 particles seem to remain at the grain boundaries.

The porosity is because most ZrO_2 particles are not homogeneously distributed between grain boundaries and Al_2O_3 particles, mainly due to lack of sufficient pressure (see Fig. 3 (A1, B1)). At a higher magnification in Fig. 3 (A2), the ZrO_2 particles appear brighter. Most of these particles failed to fill the voids among the Al_2O_3 particles, and they clustered over the bigger particles. At the same magnification of the ZrO_2 sample shown in Fig. 3 (B2) with increasing the pressure, ZrO_2 particles are shown as the small particles using ETD. More gaps were filled with these particles due to the increased pressure, causing less clustering over the Al_2O_3 matrix.

SEM micrographs of the Alumina-NCLC composites that incorporate with NCLC in 26.6% weight percent with respect to Alumina at two different pressure 40 MPa (C1, D1) and 50 MPA (C2, D2) with two magnifications of 50 µm and 10 µm are shown in Fig. 4. The microstructure demonstrated by the SEM micrographs indicated that the gra in size range is between (46 nm – 4 µm). Due to the high-performance polymer (HPP) presence in the NCLC composite, this composite had a different texture than the Al_2O_3/ZrO_2. From the first glance at both figures for the same magnification of 50 µm, it can be seen that the structure is more consistent with less porosity and voids for the 50 MPa sample. At a magnification of

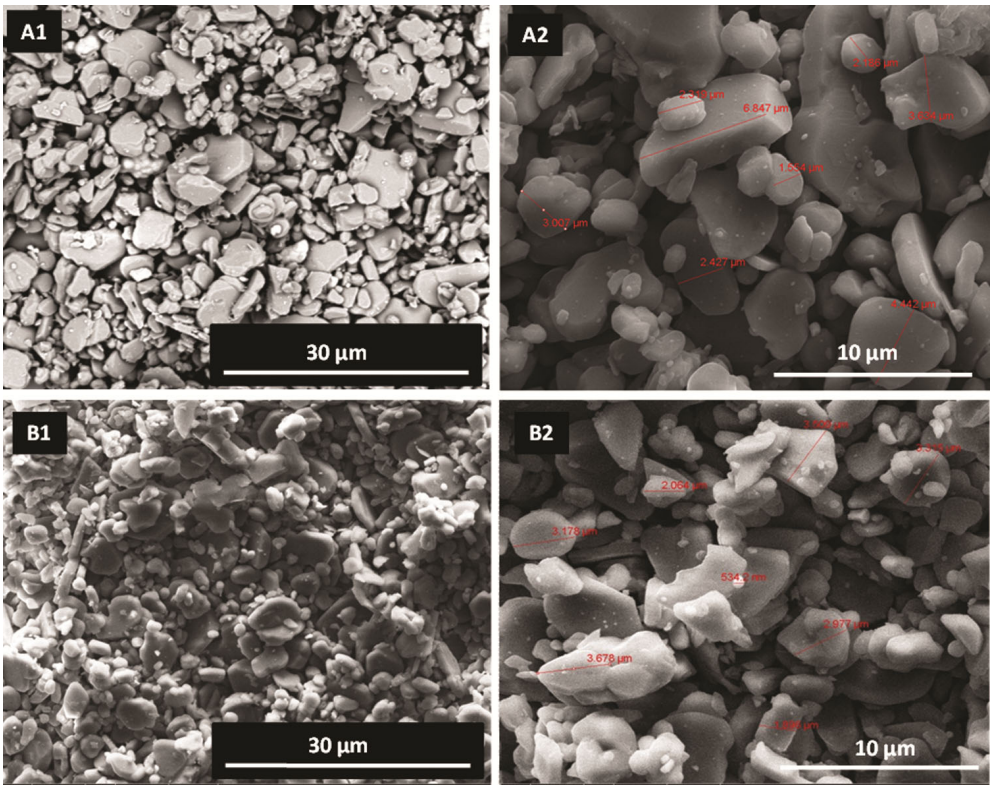

Fig. 3 — SEM micrographs of the Alumina–zirconia composites incorporated with ZnO_2 in 10% weight percent with respect to Alumina at two different pressure 40 MPa (A1, B1) and 50 MPA (A2, B2). Two magnifications of 30 µm (A1, B1) and 10 µm in (A2, B2).

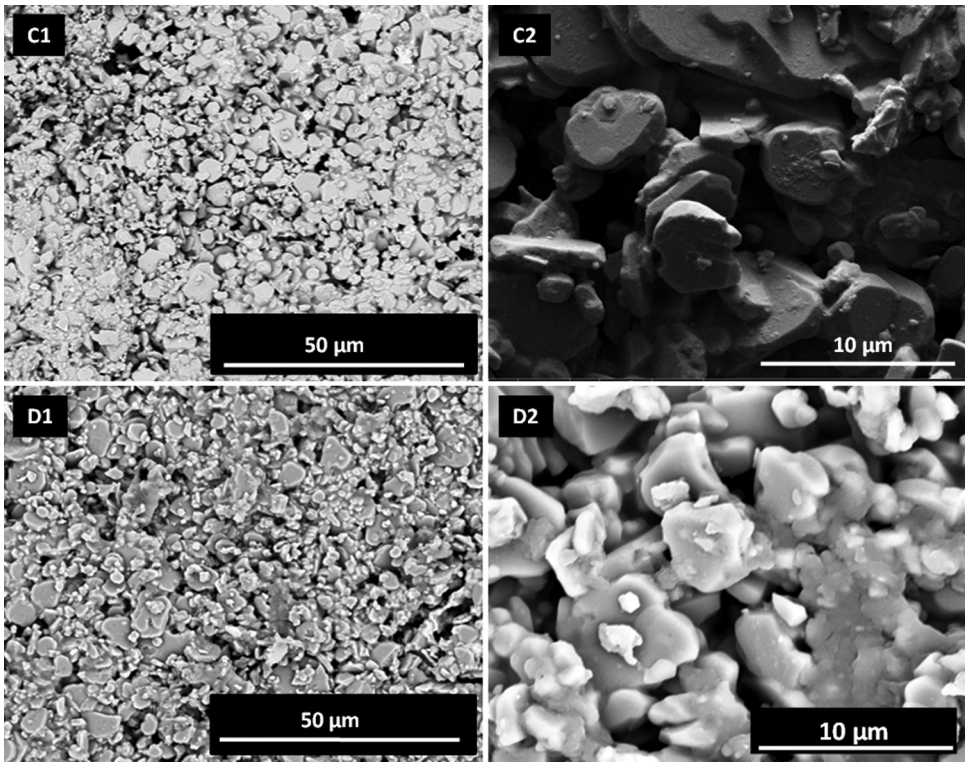

Fig. 4 — SEM micrographs of the Alumina– NCLC composites that incorporate with NCLC in 26.6% weight percent with respect to Alumina at two different pressure 40 MPa (C1, D1) and 50 MPA (C2, D2). Two magnifications of 50 µm (C1, D1) and 10 µm in (C2, D2).

10 µm, higher agglomeration is noticed. The HPP polymer filled the gaps between the particles and the grain boundaries, which worked as a binder between the composite particles. The Alumina-NCLC composites have lower porosity, cracks, and defects than Alumina-ZrO_2 composites.

3.2 Hardness scratch test

The Mohs hardness test is used to measure the scratch hardness of the samples. According to the Mohs scale, hardness scratch test results for the NCLC and ZrO_2 samples are shown in Tables 2 and 3. It can be observed that with the increase of zirconia content, the hardness of the composites slightly increases (Table 1). However, results showed that the hardness was lower than the expected threshold. The threshold was determined empirically by testing an actual ceramic plate from body armor under the same conditions for samples. The real ceramic plate resulted in hardness of 7.49 on the Mohs scale. One final thought is that ZrO_2 samples did not form enough bonding with the base ceramic material without using a binder. Therefore, higher contents lead to ZrO_2 particles agglomeration, increased porosity, decreased hardness, and ultimately poor performance. This decline in the hardness is also attributed to the decrease in the relative density of the composite. Table 3 shows the hardness of the AL_2O_3/NCLC samples. These composites show a similar tendency; the composites'

Table 2 — Hardness of the AL2O3/ZnO_2samples compared to a threshold (average of replications).

Sample ID	Sample (given in terms of additive concentration and applied pressure)	Hardness (Mohs Scale)
1	7.5% (40 MPa)	1.9
2	10% (50 MPa)	2.25
3	15% (40 MPa)	2.75
	Standard Ceramic plate	7.49
4	7.5% (50 MPa)	2.2
5	10% (40MPa)	2.45
6	15% (50MPa)	3.1

Table 3 — Hardness of the AL_2O_3/NCLC samples compared to a threshold (average of replications).

Sample ID	Sample (given in terms of additive concentration and applied pressure)	Hardness (Mohs Scale)
7	13.5% (40 MPa)	5.50
8	13.5% (50 MPa)	5.75
9	16.6% (40 MPa)	7.40
	Standard Ceramic plate	7.49
10	16.6% (50 MPa)	7.65
11	40% (40MPa)	7.65
12	40% (50MPa)	7.80

hardness levels increase with the increasing addition of NCLC content. Three of the samples achieved higher hardness than the expected threshold. The Mohs hardness of the Alumina-NCLC composite samples prepared at 40 MPa shows a slightly lower value than Alumina's hardness (Fig. 5). The hardness of the prepared sample under 50 MPa is higher than the expected threshold, which is an indication that NCLC has the potential to enhance the performance of the ceramic insert.

3.3 Data analysis for hardness test

Hardness is the main response studied in this research, a key and crucial property for the body armor's functionality. A complete randomized mixed-level full factorial design was employed. Data collected were analyzed to investigate the significant factors and obtain regression for the response. For each additive material, a total of 12 experiments (runs) were carried out, which consists of 6 different levels combinations and two replications for each.

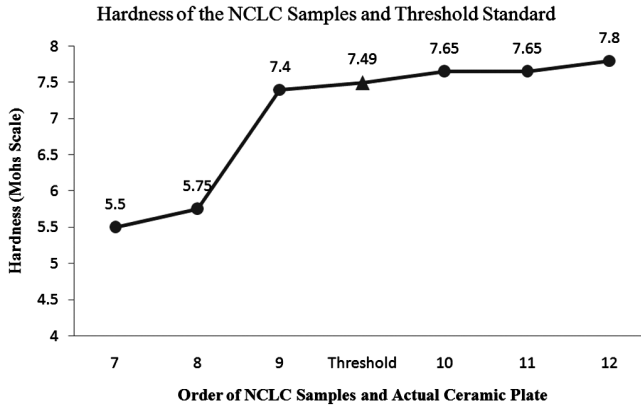

Fig. 5 — Hardness plot of the AL_2O_3/NCLC composite samples with different concentrations.

Hardness was measured and recorded as shown in Tables 2 and 3, and results were analyzed using Minitab software. Results show that both factors affect the specimen's hardness for both additives, ZrO_2 and the NCLC composite. However, there was no interaction detected between factors for both cases. Analysis of variance (ANOVA) was performed to test the significance of each factor in affecting hardness. The analysis was done based on a significance level of 0.05 (α =5%). The null and alternative hypothesis for each factor (and interaction) can be described as follows:

H_0: The factor does not affect the hardness of the material

H_1: The factor affects the hardness of the material

Analysis of variance table for the AL_2O_3/ZrO_2 is shown in Fig. 6. Results show that the p-values were 0.002 and 0.000 for pressure and additive concentration, respectively. Both are way less than the specified α value; consequently, there is strong statistical evidence to reject the null hypothesis in favor of the alternative hypothesis and conclude that both factors affect the material's hardness independently. This result means that both factors have main effects on the response, as shown in Fig. 7a. In terms of factors' interaction, the p-value for (pressure * concentration) interaction was 0.562, implying that there is no strong statistical evidence to reject the null hypothesis, which means that there is no effect for the factors 'interaction on the hardness value.

Figure 7a shows the main effect plot of both pressure and concentration on the response (Hardness value). The horizontal axis represents the two

ANOVA: Hardness (Mohs Scale) versus Pressure (MPa) and Concentrationof ZrO_2 additive% (gram/gram)

```
Factor         Type   Levels  Values
Pressure       fixed       2  40, 50
Concentration  fixed       3  7.5, 10.0, 15.0


Analysis of Variance for Hardness, using Adjusted SS for Tests

Source                 DF   Seq SS   Adj SS   Adj MS      F      P
Pressure                1  0.24083  0.24083  0.24083  26.27  0.002
Concentration           2  1.58167  1.58167  0.79083  86.27  0.000
Pressure*Concentration  2  0.01167  0.01167  0.00583   0.64  0.562
Error                   6  0.05500  0.05500  0.00917
Total                  11  1.88917


S = 0.0957427   R-Sq = 97.09%   R-Sq(adj) = 94.66%
```

Fig. 6 — ANOVA of hardnessfor AL_2O_3/ZrO_2.

different parameters' levels, and the vertical axis represents the hardness value in the Mohs scale. It is seen that an increase in pressure or concentration will increase the hardness value separately. On the other hand, the interaction plot shown in Fig. 7b indicates no interaction effect on the two factors (pressure and concentration) on hardness.

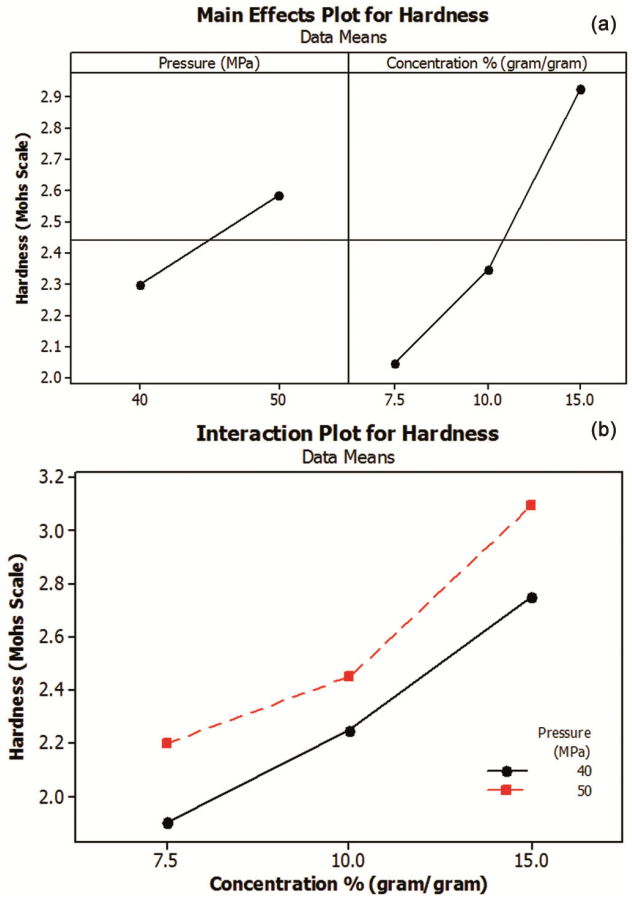

Fig. 7 — (a) Hardness main effects plot of pressure and concentration (AL_2O_3/ZrO_2) and (b) the interaction plot of the hardness (Mohs scale) as a function of the concentration of the alumina-ZrO_2 composites at different pressures.

Analysis of variance table for NCLC is shown in Fig. 8. Results show that the p-values were 0.003 and 0.000 for pressure and additive concentration, respectively. Both are significantly less than 0.05 (the α value). Consequently, there is strong statistical evidence to reject the null hypothesis in favor of the alternative hypothesis and conclude that both factors affect the sample hardness independently (i.e., they have main effects on the response), as shown in Fig. 9a. In terms of factors' interaction, the p-value for "pressure * concentration "is 0.593, implying that there is no effect on the interaction of factors on the ceramic hardness, seen from the interaction plot Fig. 9B. Regression analysis for the (AL_2O_3/NCLC) depicted in Fig. 10 shows that a linear model is a good representation of the ceramic samples' hardness in terms of both factors (NCLC concentration and pressure). The R-sq(adj) is a good indication of the model; however, it could be more accurate. Two main points to discuss in this analysis. First, the fitted model quality could be improved if more samples are tested. In this kind of experiment, samples are difficult and time-consuming to prepare. The resulted analysis is reasonably enough for drawing tentative conclusions. However, it requires a bigger sample size for more robust statistical results. Second, even though the pressure affects hardness, as mentioned in the main effect analysis, its p-value in the regression model is more than 0.05, which implies that it is not useful in predicting the hardness. This result can be explained by the small variation in hardness when increasing the pressure from 40 to 50 MPa.

ANOVA: Hardness (Mohs Scale) versus Pressure (MPa) and Concentration of NCLC Additive % (gram/gram)

```
Factor          Type   Levels  Values
Pressure        fixed       2  40, 50
Concentration   fixed       3  13.3, 26.6, 40.0


Analysis of Variance for Hardness, using Adjusted SS for Tests

Source                  DF   Seq SS   Adj SS  Adj MS       F      P
Pressure                 1   0.1408   0.1408  0.1408   24.14  0.003
Concentration            2  10.7467  10.7467  5.3733  921.14  0.000
Pressure*Concentration   2   0.0067   0.0067  0.0033    0.57  0.593
Error                    6   0.0350   0.0350  0.0058
Total                   11  10.9292


S = 0.0763763   R-Sq = 99.68%   R-Sq(adj) = 99.41%
```

Fig. 8 — ANOVA of hardness for AL_2O_3/NCLC.

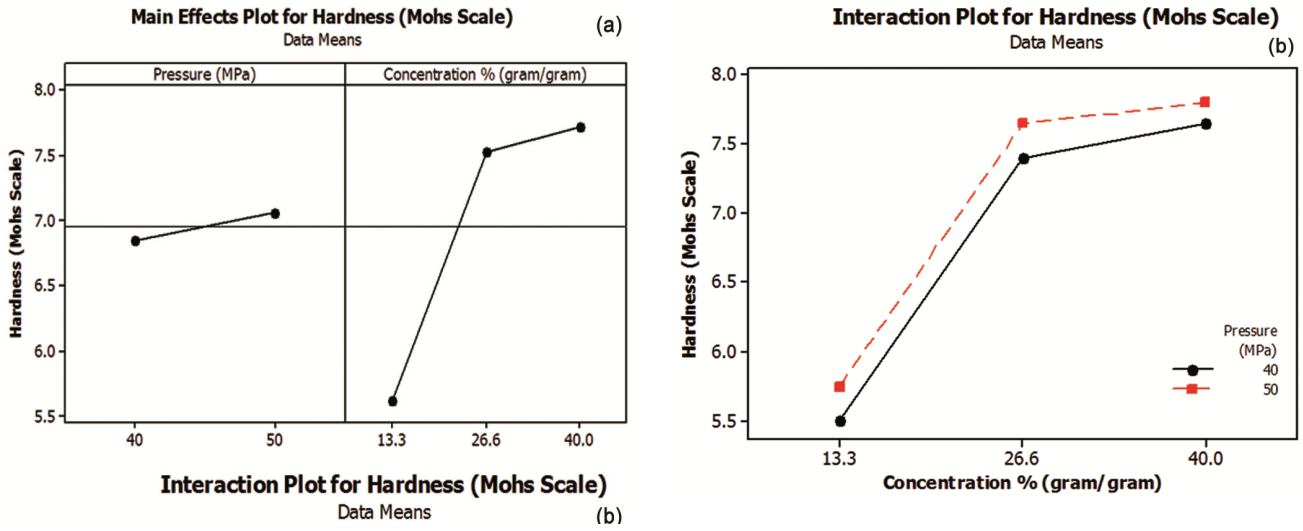

Fig. 9 — (a) Hardness main effectsplot of pressure and concentration (AL2O3/NCLC) and (b) interaction plot of the hardness (Mohs scale) as a function of the alumina- NCLC composites' concentration at different pressures.

Regression Analysis: Hardness (Mohs Scale) versus Pressure (MPa), Concentrationof NCLC % (gram/gram)

```
The regression equation is
Hardness = 3.89 + 0.0217 Pressure + 0.0786 Concentration


Predictor          Coef  SE Coef     T      P
Constant          3.891    1.272  3.06  0.014
Pressure        0.02167  0.02712  0.80  0.445
Concentration   0.07857  0.01244  6.32  0.000


S = 0.469775   R-Sq = 81.8%   R-Sq(adj) = 77.8%
```

Fig. 10 — Regression analyses (AL_2O_3/NCLC).

4 Conclusions

Different NCLC and ZrO_2 concentrations were added to Alumina under selected pressure values and investigated in this work to be used as body armor. Compositions were characterized using both SEM and X-ray diffraction. Compared to the NCLC composite, the ZnO_2 microstructure shows defects and cracks that can substantially reduce the armor-related properties such as hardness. The Mohs hardness test was used for the composition's hardness characterization. The Alumina-NCLC composites' analysis has shown that the NCLC addition promotes composite with higher hardness. ANOVA was utilized to evaluate the reliability of the obtained results. According to the obtained results, the compositions with NCLC showed comparable results with each other and higher hardness than a composition with ZrO_2. This observation was a good indication that the addition of NCLC to Alumina enhances the microstructure and increases the Ceramic's hardness, resulting in an overall improvement in Ceramic's body armor application performance.

Acknowledgments

The authors are grateful for the "King Abdullah II Fund for Development (KAFD)" and "King Abdullah II Design and Development Burea (KADDB)" for the grant and support on this project. Grant number (28/2018). The role of the sponsors of this project, KAFD, and KADDB, was to pay for the materials and testing expenses. They have no part in collecting data, analyzing results, and interpreting the results. A special thank goes to Eng. Abdullah Alshboul from Jordan University of Science and Technology for his support. Finally, we offer our appreciation to the Geology and physics departments at The University of Jordan for their help and support in their labs.

References

1 National Research Council, Opportunities in Protection Materials Science and Technology for Future Army Applications (The National Academies Press, Washington DC), 1st Edn, ISBN-13: 978030921285 4, (2011).

2 Benzait A & Trabzon L, *J Compos Mater,* 52 (2018) 3241.

3 Medvedovski E, Silicon Carbide-Based Ceramics for Ballistic Protection (Ceramic Armor and Armor Systems, Wiley Online Library), Vol 151, ISBN: 9781118406793, 2003, p. 19.

4 McCauley J W, Crowson A, Gooch Jr W A, Rajendran A M, Bless S J, Logan K, Normandia M & Wax S, Ceramic Armor Materials by Design (John Wiley & Sons), Vol 134, ISBN 1 57498 148 X, (2012).

5 Lamba O S, Nangru S C, Joshi L M, Sharma A, Singh V V P & Gupta N C, *Indian J Eng Mater Sci,* 7 (2000) 443.

6 Medvedovski E, *Ceram Int,* 36.7 (2010) 2103.

7 Crouch I G, Appleby-Thomas G & Hazell P J, *Int J Impact Eng,* 80 (2015) 203.

8 Carter A B & Norton M G, Ceramic Materials: Science and Engineering (Springer, New York), 2nd Edn, ISBN: 978 1 4614 3523 5, (2013).

9 Groover M P, Fundamentals of Modern Manufacturing: Materials, Processes, and Systems (John Wiley & Sons, Inc., NJ), 4th Edn, ISBN: 978 0470 467002, 2010, p. 258.

10 Karandikar P G, Evans G, Wong S, Aghajanian M K & Sennett M, *Advances in Ceramic Armor IV*, 29 (2009) 163.

11 Raigrodski A J, *J Prosthet Dent,* 92 (2004) 557.

12 Liang X F, Yin G F, Yang S Y & Wang J X, *West China J Stomatology,* 24 (2006) 303.

13 Milosevic M, *Procedia Engineer,* 149 (2016) 313.

14 Mallick P K, Processing of Polymer Matrix Composites(CRC Press Florida), 1st Edn, ISBN: 978 1 4665 7822 7, (2017).